THE JOURNAL OF BIOLOGICAL CHEMISTRY
Vol. 277, No. 23, Issue of June 7, pp. 20264–20269, 2002
Printed in U.S.A.

Biochemical Characterization of the Kinase Domain of the Rice Disease Resistance Receptor-like Kinase XA21*

Received for publication, November 16, 2001, and in revised form, March 27, 2002
Published, JBC Papers in Press, April 1, 2002, DOI 10.1074/jbc.M110999200

Guo-Zhen Liu‡, Li-Ya Pi‡, John C. Walker§, Pamela C. Ronald¶, and Wen-Yuan Song‡‖

From the ‡Department of Plant Pathology, University of Florida, Gainesville, Florida 32611, the §Division of Biological Sciences, University of Missouri, Columbia, Missouri 65211, and the ¶Department of Plant Pathology, University of California, Davis, California 95616

The rice disease resistance gene, *Xa21*, encodes a receptor kinase-like protein consisting of leucine-rich repeats in the putative extracellular domain and a serine/threonine kinase in the putative intracellular domain. The putative XA21 kinase domain was expressed as maltose-binding and glutathione *S*-transferase fusion proteins in *Escherichia coli*. The fusion proteins are capable of autophosphorylation. Phosphoamino acid analysis of the glutathione *S*-transferase fusion protein indicates that only serine and threonine residues are phosphorylated. The relative phosphorylation rate of the XA21 kinase against increasing enzyme concentrations follows a first-order rather than second-order kinetics, indicating an intramolecular phosphorylation mechanism. Moreover, the active XA21 kinase cannot phosphorylate a kinase-deficient mutant of XA21 kinase. The enzymatic activity of the XA21 kinase in a buffer containing Mn^{2+} is at least 15 times higher than that with Mg^{2+}. The K_m and V_{max} of XA21 kinase for ATP are 0.3 μM and 8.4 nmol/mg/min, respectively. Tryptic phosphopeptide mapping reveals that multiple sites on the XA21 kinase are phosphorylated. Finally, our data suggest that the region of XA21 kinase corresponding to the RD kinase activation domain is not phosphorylated, revealing a distinct mode of action compared with the tomato Pto serine/threonine kinase conferring disease resistance.

Plants are continually under attack by a variety of pathogens and have developed a wide array of defense mechanisms to protect themselves. Genetic analyses of plant-pathogen interactions have revealed that the resistance reactions, in many cases, are controlled by two dominant loci: an avirulence (avr) gene in the pathogen and a corresponding resistance (R) gene in the plants. Lack of either gene results in the development of disease symptoms. These genetic interactions are defined by the gene-for-gene theory (1).

A number of plant R genes, which confer gene-for-gene type resistance, have been cloned and characterized from diverse plants. The encoded proteins can be grouped into six classes based on structure: a serine/threonine kinase, proteins with a nucleotide-binding site and leucine-rich repeats (LRR),[1] presumed extracellular LRR-containing proteins with or without a transmembrane domain, a serine/threonine receptor-like kinase (RLK), and a protein without significant homology to known proteins (2–5).

Among all of the cloned resistance genes, only two encode protein kinases. The tomato *Pto* gene conferring resistance to *Pseudomonas syringae* pv. *tomato* containing the *avr* gene *avrPto*, encodes a serine/threonine kinase (Pto) that interacts with avrPto and several other proteins known as Ptis (6–10). The Pto kinase can autophosphorylate eight serine and threonine residues and the autophosphorylation proceeds via an intramolecular mechanism (11, 12). The predicted amino acid sequence of Pto indicates that it belongs to a large subfamily of protein kinases known as RD kinases, which have an arginine immediately preceding the conserved catalytic aspartate (13). Consistent with other RD kinases whose activation requires phosphorylation of the activation domain, a region spanning the conserved sequences DFG and PE (13), Pto autophosphorylates its activation domain *in vitro* (12). Moreover, specific amino acid substitutions in this region result in constitutive induction of the hypersensitive response in the absence of *avrPto* (14).

The rice bacterial blight disease resistance gene, *Xa21*, encodes a RLK protein (15). The putative extracellular domain is composed of 23 LRRs, whereas the putative intracellular domain (XA21K) contains all the invariant amino acid residues characteristic of serine/threonine protein kinases. Based on the mode of action of animal receptor-tyrosine kinases (RTKs), we have hypothesized that the XA21 LRR domain acts as receptor for a plant or pathogen-produced ligand and that upon ligand binding, XA21K undergoes autophosphorylation by an intra- or intermolecular mechanism (16). In this report, we demonstrate that XA21K is an active serine/threonine kinase, that autophosphorylation of multiple residues occurs exclusively via an intramolecular mechanism, and that the XA21K region corresponding to the RD kinase activation domain is not phosphorylated.

EXPERIMENTAL PROCEDURES

Construction of XA21K Expression Plasmids—XA21K (amino acids 677–1025) (15) was PCR-amplified with primer 1 (5′-GGATCCGCACAAGAGAACTAAAAAGGGAGC-3′) and primer 2 (5′-CAGAAGTCGATCTGAAGTGTGGCA-3′), cloned, sequenced to confirm that no PCR error was introduced, and subcloned into the pGTK vector, which was

* This work was supported by National Science Foundation Grant 0080155 and a visiting fellowship for inter-laboratory research from the Multi-Institutional Plant Protein Phosphorylation Group (to W.-Y. S.) and a grant from the National Institutes of Health (to P. C. R.). This is Florida Agricultural Experiment Station Journal Series number R-08639. The costs of publication of this article were defrayed in part by the payment of page charges. This article must therefore be hereby marked "*advertisement*" in accordance with 18 U.S.C. Section 1734 solely to indicate this fact.

‖ To whom correspondence should be addressed: Dept. of Plant Pathology, University of Florida, 1453 Fifield Hall, Gainesville, FL 32611-0680. Tel.: 352-392-3631 (ext. 344); Fax: 352-392-6532; E-mail: wsong@mail.ifas.ufl.edu.

[1] The abbreviations used are: LRR, leucine-rich repeats; GST, glutathione *S*-transferase; MBP, maltose-binding protein; RLK, receptor-like kinase; RTK, receptor-tyrosine kinase; XA21K, XA21 kinase; PP1, protein phosphatase 1.

modified from pGEX-2T (Amersham Biosciences) (17). The resulting plasmid was designated as pGST-XA21K and used for protein expression.

A single amino acid mutation in XA21K was introduced using the method of Deng and Nickoloff (18). Two primers (primer 3, 5′-GGACTTGGTTGAATACTCACCAG-3′; primer 4, 5′-AAGCTTTAGTACCTCCACTGCAACA-3′) were designed to introduce mutations in the vector for mutant selection and also to substitute the lysine 736 (Lys-736) codon of XA21K. The lysine mutation creates a single substitution of glutamic acid for Lys-736. Candidates were confirmed by DNA sequencing and cloned into the pGTK vector. The resulting construct, designated pGST-XA21K-K736E, was used to express the kinase-deficient form of XA21K.

To express XA21K as a maltose-binding protein (MBP) fusion protein, plasmids pMBP-XA21K and pMBP-XA21K-K736E were created. Primer 5 (5′-GGATCCGTCGACCACAAGAGAACTAAAAAGGGAGC-3′) and primer 6 (5′-GGATCCGTCGACCCCGGGCAGAAGTCGATCTGAAGTGTGGCA-3′) were used to amplify XA21K and its kinase-deficient mutant using pGST-XA21K and pGST-XA21K-K736E as templates. The PCR products were cloned into the pMal-c2X expression vector (New England Biolabs, Beverly, MA) and confirmed by sequencing.

All other XA21K mutants used in this study were created according to the methods from Stratagene (La Jolla, CA). pGST-XA21K was used as a template. Primer pairs S(−8)A-For (5′-GCAAGAAGAGCAGCTGTGGAATTCCCG-3′)/S(−8)A-Rev (5′-CGGGAATTCCACAGCTGCTCTTCTTGC-3′), S(−21)A-For (5′-GATCTGGTTCCGCGGGGAGCCGACTACAAAGAC-3′)/S(−21)A-Rev (5′-GTCTTTGTAGTCGGCTCCCCGCGGAACCAGATC-3′), R865H-For (5′-GATTTTGGGCTTGCACACATACTAGTTGATGGGACCTC-3′)/R865H-Rev (5′-GAGGTCCCATCAACTAGTATGTGTGCAAGCCCAAAATC-3′), and H903R-For (5′-GCTCATTGCATCAACGCGTGGAGATATTTACAGC-3′)/H903R-Rev (5′-GCTGTAAATATCTCCACGCGTTGATGCAATGAGC-3′) were used to generate the S(−8)A, S(−21)A, R865H, and H903R mutants, respectively.

Expression and Purification of Fusion Proteins—pMBP-XA21K and pMBP-XA21K-K736E were transformed into *Escherichia coli* strain ER2566 (New England Biolabs). Bacterial cells were grown in 50 ml of LB supplemented with glucose (2 g/liter) and ampicillin (50 μg/ml) to A_{600} of 0.5–0.6. To induce expression of the fusion proteins, isopropyl-1-thio-β-D-galactopyranoside was added to a final concentration of 0.4 μM and incubated for 8 h at room temperature. Cells were harvested by centrifugation, resuspended into column buffer (20 mM Tris-HCl (pH 7.4), 200 mM NaCl, 1 mM EDTA), supplemented with phenylmethylsulfonyl fluoride (2 mM) and dithiothreitol (1 mM), and lysed by sonication followed by gentle agitation at 4 °C for 10 min. The lysate was centrifuged (14,000 × *g*) for 10 min at 4 °C. The supernatant was mixed with 60 μl of amylose resin (New England Biolabs) followed by incubation for 1 h at 4 °C. After washing with column buffer extensively, the fusion protein was eluted with column buffer containing 3.6 mg/ml maltose.

A similar protocol was used to express and purify GST-XA21K and GST-XA21K-K736E except that a shorter time period (40 min) was used for isopropyl-1-thio-β-D-galactopyranoside induction and that the GST buffer (50 mM HEPES (pH 7.4), 150 mM NaCl, 10 mM EDTA, 1 mM dithiothreitol) and glutathione-agarose beads (Sigma) were used for purification.

Autophosphorylation and Dephosphorylation Assays—The resin-bound fusion proteins purified above were washed with kinase buffer (50 mM HEPES (pH 7.4), 10 mM $MgCl_2$, 10 mM $MnCl_2$, 1 mM dithiothreitol). Autophosphorylation experiments were carried out in a 30-μl reaction mixture containing 20 μl of resin-bound protein (5 μg) and 20 μCi of [γ-^{32}P]ATP (6000 Ci/mmol) (PerkinElmer Life Science, Boston, MA). The reaction was stopped after 30 min by adding 10 μl of Laemmli loading buffer (×4) and boiling for 5 min. The proteins were separated by SDS-PAGE (7.5 or 10%). After staining with Coomassie Brilliant Blue G-250, the gel was dried and exposed to x-ray film.

To dephosphorylate the phosphorylated fusion proteins, the ^{32}P-labeled XA21K proteins were washed with protein phosphatase 1 (PP1) buffer and incubated with PP1 (New England Biolabs) according to the manufacturer's protocol. The resulting proteins were resolved by SDS-PAGE as described above.

For the divalent cation dependence and time course assays, the indicated amount of MBP-XA21K was mixed with 10 μCi of [γ-^{32}P]ATP in a total volume of 20 μl of kinase buffer and divalent cation-containing buffer, respectively. For ATP dependence assays, 2 μg of fusion protein was incubated with 0.1–50 μM cold ATP containing 3.75 μCi of [γ-^{32}P]ATP in a total volume of 30 μl of kinase buffer and stopped at 15 min by adding 10 μl of Laemmli loading buffer (×4). One-half of the reaction was separated by SDS-PAGE. The Coomassie Blue-stained protein bands were recovered and then measured using a scintillation counter. ATP incorporation was calculated based on the radioactivity counts and the concentration of cold ATP. K_m and V_{max} were estimated according to the double-reciprocal plot and linear regression using SigmaPlot 2000 V6 software (SPSS Inc., Chicago, IL). The intramolecular phosphorylation assays were performed according to the method described by Sessa *et al.* (11) with some modifications. Increased amounts of fusion proteins (from 0.7 to 44.8 μM) were used to incubate with 5 μCi of [γ-^{32}P]ATP. The reactions were stopped at 10 min by adding an equal volume of 75 mM H_3PO_4. One-half of the reaction was spotted on P-81 phosphocellulose paper. The incorporated ^{32}P was determined as described above. Van't Hoff analysis and linear regression was carried out using SigmaPlot 2000 V6 software (SPSS Inc.).

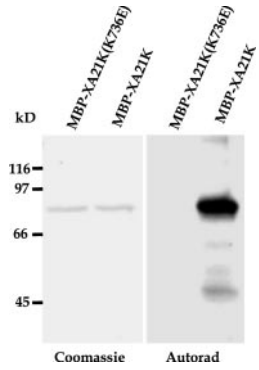

FIG. 1. **Autophosphorylation of MBP-XA21K and MBP-XA21K-K736E.** Equal amounts of affinity-purified proteins were incubated with [γ-^{32}P]ATP in the kinase buffer described under "Experimental Procedures" for 30 min at room temperature. Samples were then resolved by 10% SDS-PAGE gel. Both the Coomassie Blue-stained gel (*left*) and autoradiogram (*right*) of the same gel are shown.

Phosphoamino Acid Assays—The phosphoamino acid assay was carried out according to Horn and Walker (19). The autophosphorylated GST-XA21K was excised from the gel and extracted with 50 mM NH_4HCO_3 (pH 8.3), 0.1% SDS, and 0.5% 2-mercaptoethanol. The recovered protein was then precipitated with 20% (w/v) trichloroacetic acid. The ^{32}P-labeled fusion protein was hydrolyzed in 50 μl of 6 N HCl (Pierce) for 1 h at 110 °C. HCl was removed by vacuum centrifugation and the pellet was dissolved in pH 1.9 buffer (2.2% formic acid, 7.8% acetic acid, and 100 μg/ml each phosphoamino acids standards (Ser(P), Thr(P), and Tyr(P)) (Sigma)). The sample was loaded onto a 20 × 20-cm thin-layer cellulose (TLC) plate (C.B.S. Scientific Co., Del Mar, CA) and subjected to electrophoresis (horizontally at pH 1.9, 1.5 kV for 30 min and vertically at pH 3.5, 1.3 kV for 25 min) using a Hunter thin layer electrophoresis system, model number HTLE7000 (C.B.S. Scientific Co.). After spraying with 0.25% ninhydrin in acetone to visualize the standard phosphoamino acids, the plate was subjected to autoradiography.

Phosphopeptide Mapping—For phosphopeptide mapping, the recovered ^{32}P-labeled fusion protein was oxidized in 50 μl of cold performic acid for 60 min. The performic acid was removed with vacuum centrifugation and the pellet was resuspended in 50 μl of 50 mM NH_4HCO_3 (pH 8.3), and digested overnight with L-1-tosylamido-2-phenylethyl chloromethyl ketone-treated trypsin (Worthington) at 37 °C. After repeated drying and resuspension in water for three times, the sample was dissolved in pH 1.9 buffer and loaded onto a TLC plate. The tryptic phosphopeptides were resolved by electrophoresis in the first dimension (pH 1.9, 1.5 kV, 40 min) followed by ascending chromatography about 12 h in phosphopeptide buffer (75:50:15:60, *n*-butanol:pyridine:acetic acid:water). The plate was subjected to autoradiography to visualize the phosphopeptides.

RESULTS

XA21K Is a Functional Kinase—To test the hypothesis that *Xa21* encodes a protein kinase, we expressed and purified XA21K as a MBP recombinant fusion protein and assayed for autophosphorylation. Fig. 1 shows that the fusion protein (MBP-XA21K) is capable of autophosphorylation.

To confirm that the phosphorylated protein was MBP-XA21K rather than a contaminating bacterial protein, a mutated MBP-XA21K construct was generated using the site-directed mutagenesis approach. A single base substitution replaced Lys-736 with a glutamic acid residue. Because Lys-

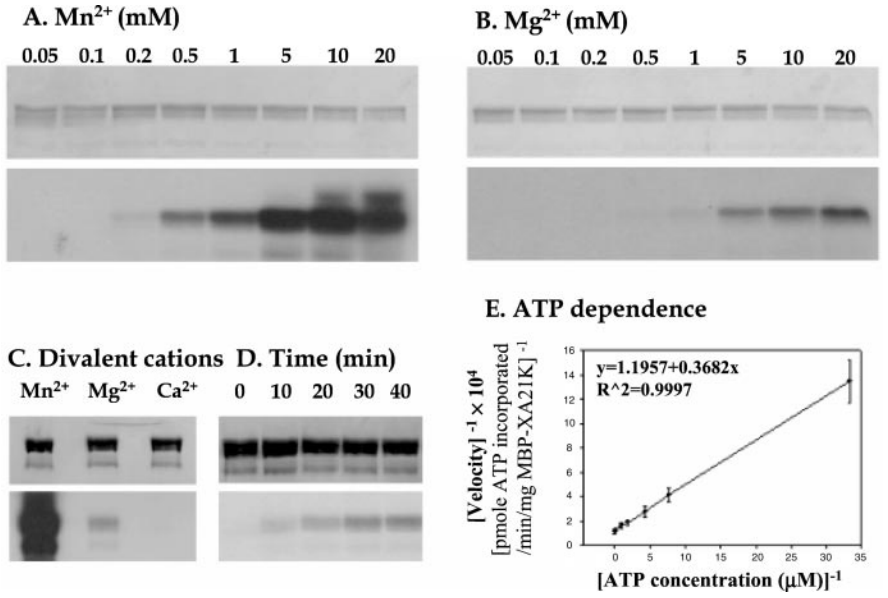

FIG. 2. **Enzymatic properties of XA21K.** Autophosphorylation of MBP-XA21K was carried out for 30 min at room temperature in kinase buffer containing different concentrations of $MnCl_2$ (*A*), $MgCl_2$ (*B*), and 10 mM of distinct divalent cations (*C*). Time course experiments of MBP-XA21K were performed with 10 mM $MnCl_2$ and 10 mM $MgCl_2$ (*D*). Samples were then resolved by 10% SDS-PAGE. Both the Coomassie Blue-stained gel (*upper*) and autoradiogram (*lower*) of the same gel are shown. *E*, the kinetics of XA21K autophosphorylation with respect to ATP. The double-reciprocal plot showed that the K_m and V_{max} are 0.3 μM and 8.4 nmol/mg/min, respectively.

736 is essential for phosphotransfer and highly conserved in all protein kinases, the K736E mutation is expected to inactivate XA21K. Indeed, autophosphorylation analysis of the MBP-XA21K-K736E mutant revealed no autophosphorylation activity (Fig. 1). Similar results were observed when XA21K was expressed as GST fusion protein (data not shown). Because MBP and GST alone do not have any detectable kinase activity, these results indicate that *Xa21* encodes an active kinase capable of autophosphorylation *in vitro*.

Characterization of XA21K—The kinase activity of XA21K requires the presence of divalent cations. A linear increase in the enzymatic activity of XA21K was observed in the range of 0.1–5 mM $MnCl_2$, followed by a plateau of the autophosphorylation when the concentration of $MnCl_2$ was further increased (Fig. 2*A*). Magnesium chloride maintains the linear increase of the autophosphorylation up to the highest concentration (20 mM) used in this assay (Fig. 2*B*). The kinase activity of XA21K was, however, at least 15 times higher in the presence of $MnCl_2$ than in $MgCl_2$ (Fig. 2*C*). No detectable kinase activity was observed when $CaCl_2$ was used as a source of divalent cation. Time course experiments with 10 mM $MnCl_2$ and $MgCl_2$ indicated that the autophosphorylation of XA21K reached a plateau after 30–40 min (Fig. 2*D*).

MBP-XA21K exhibits standard Michaelis-Menten kinetics with respect to ATP. The K_m and V_{max} values for ATP, determined by a double-reciprocal plot, are 0.3 μM and 8.4 nmol/mg/min, respectively (Fig. 2*E*).

XA21K Is Serine/Threonine-specific—Based on the sequence of amino acids in kinase subdomains VI and VIII, *Xa21* was presumed to encode a serine/threonine protein kinase (15). To confirm the serine/threonine specificity of XA21K, phosphoamino acid assays were performed. In these assays, serine and threonine residues were phosphorylated, whereas no detectable tyrosine residues were labeled (Fig. 3*A*). Moreover, the autophosphorylated XA21K can be dephosphorylated by the serine/threonine phosphatase PP1 (Fig. 3*B*). These results indicated that XA21K carries serine/threonine specificity.

The XA21K Autophosphorylation Occurs through an Intramolecular Mechanism—To test whether the autophosphorylation of XA21K proceeds via an intramolecular (first-order with respect to enzyme concentration) or intermolecular (second-order with respect to enzyme concentration) mechanism, the autophosphorylation reaction was carried out in the presence of increasing concentrations of XA21K. As shown in Fig. 4*A*, the relative phos-

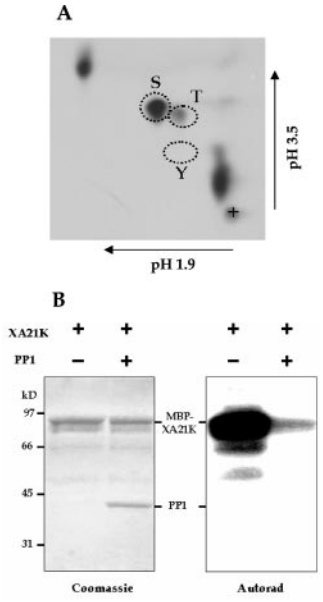

FIG. 3. **XA21K is a serine/threonine kinase.** *A*, phosphoamino acid assays of the autophosphorylated GST-XA21K. The ^{32}P-labeled GST-XA21K was hydrolyzed with HCl and subjected to two-dimensional analysis as described under "Experimental Procedures." The autoradiogram spots indicate the positions of phosphorylated serine and threonine residues. *Dashed circles* indicate the positions of standard phosphorylated serine, threonine, and tyrosine. *B*, dephosphorylation of MBP-XA21K by the serine/threonine phosphatase PP1. The ^{32}P-labeled MBP-XA21K was incubated with and without PP1 phosphatase for 30 min at room temperature. The samples were then resolved by 10% SDS-PAGE. Both the Coomassie Blue-stained gel (*left*) and autoradiogram (*right*) of the same gel are shown.

phorylation rate increases linearly with the increasing enzyme concentration. This result indicated that autophosphorylation of MBP-XA21K follows first-order rather than second-order reaction kinetics. Moreover, the phosphate incorporation per molecule of MBP-XA21K was at the same level when the MBP-XA21K concentration in the reaction varied from 0.7 to 44.8 μM (64 times) (Fig. 4*B*). The van't Hoff analysis of autophosphorylation (logarithm of phosphorylation rate *versus* logarithm of enzyme concentration) illustrated a slope of 1.03 ± 0.02 and a correlation coefficient of 0.997 for linear regression (Fig. 4*C*). Our data sug-

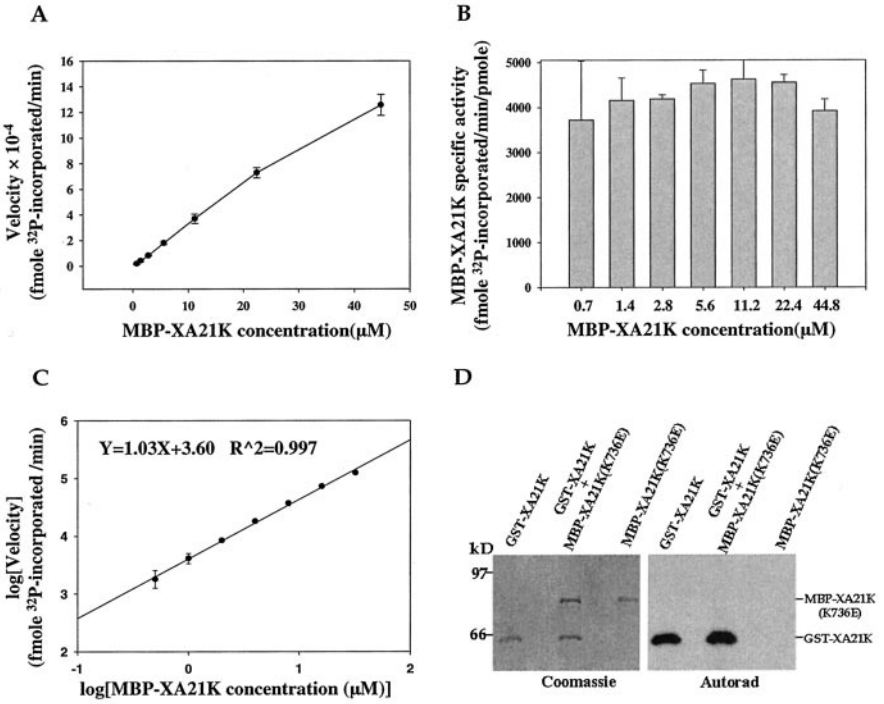

FIG. 4. **Intramolecular phosphorylation assays of the XA21K.** Increased concentrations of MBP-XA21K (from 0.7 to 44.8 μM) were used to perform autophosphorylation as described in the legend to Fig. 1. *A*, plot of phosphate incorporation rate *versus* MBP-XA21K concentration. *B*, specific activity of MBP-XA21K expressed as phosphate incorporation rate per pmol of MBP-XA21K. *C*, van't Hoff plot of log velocity *versus* the log of MBP-XA21K concentration has a slope of 1.03 ± 0.02 and a correlation coefficient of 0.997. Data in *A–C* are the mean ± S.E. (n = 3). *D*, GST-XA21K cannot transphosphorylate the kinase-deficient mutant MBP-XA21K-K736E. Free GST-XA21K was incubated with free MBP-XA21K-K736E and [γ-^{32}P]ATP in kinase buffer for 30 min at room temperature. Autophosphorylations of GST-XA21K and MBP-XA21K-K736E were performed as controls. Samples were resolved by 7.5% SDS-PAGE. Coomassie Blue staining (*left*) and autoradiogram (*right*) of the same gel are shown.

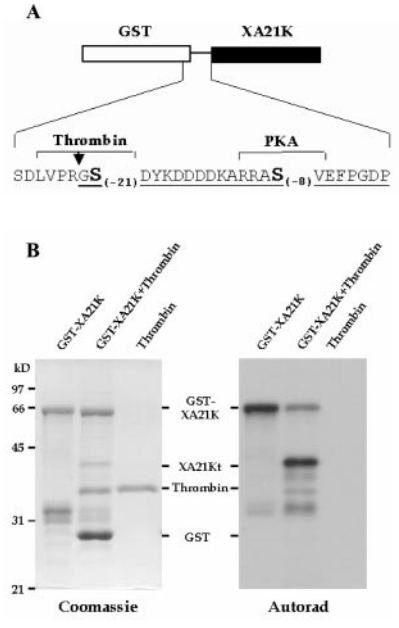

FIG. 5. **XA21K cannot phosphorylate the GST protein.** *A*, schematic diagram showing structural domains of GST-XA21K. The 22 amino acids on XA21Kt are *underlined*. S(−8) and S(−21) are shown in *bold* and *larger size*. The thrombin recognition and protein kinase A phosphorylation sites are indicated. *B*, XA21Kt released by thrombin digestion. The ^{32}P-labeled GST-XA21K was digested with thrombin at room temperature for 16 h. Both GST-XA21K and thrombin were used as controls. The samples were resolved by 10% SDS-PAGE. Coomassie Blue staining (*left*) and autoradiogram (*right*) of the same gel are shown.

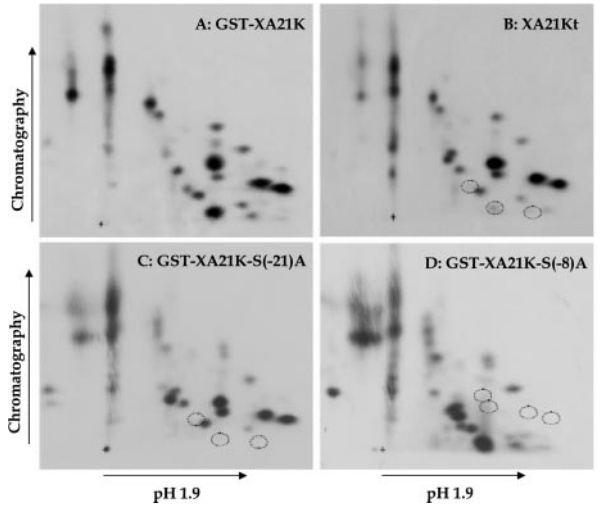

FIG. 6. **Multiple residues on XA21K are autophosphorylated *in vitro*.** The ^{32}P-labeled GST-XA21K and its mutants were digested with trypsin and subjected to two-dimensional electrophoresis and chromatography analysis as described under "Experimental Procedures." The autoradiogram spots are the phosphorylated peptides generated from trypsin digestion. The origin is indicated by "+." *A*, GST-XA21K; *B*, XA21Kt; *C*, GST-XA21K-S(−21)A; *D*, GST-XA21K-S(−8)A.

gested that the MBP-XA21K autophosphorylation occurs via an intramolecular mechanism.

To confirm that intermolecular autophosphorylation does not occur, a kinase-deficient form of XA21K (MBP-XA21K-K736E) was used as a potential substrate for phosphorylation by GST-XA21K. Free MBP-XA21K-K736E was incubated with free GST-XA21K. Consistent with the results described above, GST-XA21K was unable to transphosphorylate MBP-XA21K-K736E (Fig. 4*D*). Similar results were obtained by using GST-XA21K-K736E as a potential substrate for phosphorylation by MBP-XA21K (data not shown). These results, together with the observations from the intramolecular phosphorylation assays described above, support the notion that autophosphorylation of XA21 exclusively occurs through an intramolecular mechanism *in vitro*.

Multiple Serine/Threonine Residues on XA21K Are Autophosphorylated in Vitro—To investigate the number of autophosphorylated serine and threonine residues, phosphopeptide mapping was carried out using both GST-XA21K and the XA21K protein without GST. XA21K was released from GST-XA21K by digestion with thrombin (Fig. 5). Because the thrombin-released XA21K contains a 22-amino acid peptide derived from the GTK vector, we designated the released XA21K as

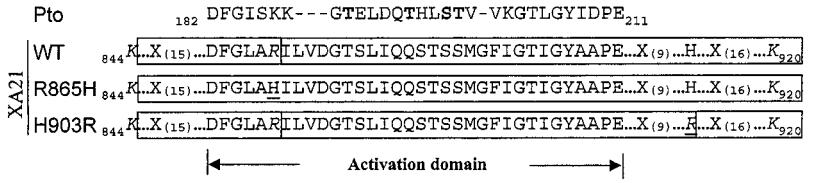

FIG. 7. **Sequence comparison of the activation domain of XA21K and Pto.** Identified phosphorylation sites on Pto (12) are in *bold*. Mutated residues in the XA21K mutants (R865H and H903R) are *underlined*. Arginine and lysine recognized by trypsin on XA21K and the mutants are indicated in *italic*. Tryptic peptides are *boxed*. *X* represents the amino acids that are not shown. − denotes gaps for maximal alignment.

XA21Kt. Bands of predicted sizes of XA21Kt and GST were observed after thrombin digestion (Fig. 5*B*). Autoradiography analysis showed that a protein with the predicted size of XA21Kt was strongly phosphorylated, indicating that this protein is XA21Kt (Fig. 5*B*). No radiolabeled products at the position corresponding to GST were found. The weak bands observed on both the Coomassie Blue-stained gel and the autoradiogram in the GST-XA21K lanes may be the results of partial degradation of XA21Kt.

Both GST-XA21K and XA21Kt were subjected to phosphopeptide mapping assays to determine the phosphopeptide pattern. The ^{32}P-labeled proteins were digested with trypsin, and the resulting peptides were loaded onto TLC plates and resolved horizontally by electrophoresis and vertically by ascending chromatography. Multiple labeled spots were observed on the autoradiograms generated from both GST-XA21K and XA21Kt (Fig. 6, *A* and *B*). Interestingly, three spots were absent in the tryptic pattern of XA21Kt when compared with that of GST-XA21K. Because the thrombin-released GST is not labeled as shown in Fig. 5*B*, we hypothesized that the absence of three GST-XA21K-specific spots was because of the cleavage of a phosphorylated residue by thrombin. Indeed, the S(−21) residue on the 22-amino acid peptide of XA21Kt is part of the thrombin recognition site (Fig. 5*A*). To test this hypothesis, we mutated S(−21) to alanine on GST-XA21K, and the mutant was subjected to phosphopeptide mapping. As shown in Fig. 6*C*, the phosphopeptide pattern of GST-XA21K-S(−21)A is identical to that of XA21Kt. This result indicates that S(−21) is phosphorylated by the XA21 kinase and also confirms that the GST portion does not contain any phosphorylation sites.

In addition to S(−21), there is another serine residue (S(−8)) located on the 22-amino acid peptide between GST and the XA21 kinase domain (Fig. 5*A*). We mutated S(−8) to alanine to test whether this residue is also phosphorylated. Phosphopeptide mapping of the GST-XA21K-S(−8)A showed that S(−8) accounts for four phosphospots as shown in Fig. 6*D*. Interestingly, S(−8) is located at the protein kinase A recognition sequence. Taken together, these results indicate that at least 20 of 27 phosphospots on the GST-XA21K peptide map are because of autophosphorylation of XA21K, thereby strongly suggesting that multiple residues on XA21K are autophosphorylated.

The Activation Domain of XA21K Does Not Carry Any Phosphorylation Sites—There are seven serine and threonine residues located in the presumed activation domain of XA21K, and all of them are included in a single tryptic peptide (Fig. 7). To determine whether any of the residues can be autophosphorylated by XA21K, we mutated arginine 865 (Arg-865) to histidine, which abolishes a trypsin recognition site upstream of the seven serine and threonine residues. Because this mutation will significantly increase the size of the tryptic peptide carrying the seven serine and threonine residues, a shift of a labeled spot(s) on the two-dimensional autoradiogram should be observed if the peptide contained a phosphorylated residue(s). However, tryptic mapping of the GST-XA21K-R865H mutant showed no detectable changes on the autoradiogram when compared with that of GST-XA21K (data not shown). To confirm this result, we further mutated histidine 903 (His-903), downstream of the activation domain, to arginine to create a new trypsin recognition site. Consistent with the result from the GST-XA21K-R865H mutant, the GST-XA21K-H903R mutant showed an identical tryptic pattern to that of the wild type GST-XA21K (data not shown). These results suggest that the activation domain of XA21K is not autophosphorylated *in vitro*.

DISCUSSION

It has long been hypothesized that protein phosphorylation plays a key role in R gene-mediated disease resistance (20). In this paper, we demonstrate that the presumed intracellular domain encoded by the rice disease resistance gene *Xa21* is an active serine/threonine kinase capable of autophosphorylation. Like other protein kinases, XA21K activity can be abolished by a single substitution of the invariant lysine residue that is responsible for phosphotransfer. The enzymatic properties of XA21K are also similar to those of other characterized kinases. For instance, the MBP-XA21K K_m for ATP (0.3 μM) is comparable with the values obtained for the epidermal growth factor receptor (0.2–3 μM), the *Catharanthus roseus* CrRLK1 (2–2.5 μM), and the *Arabidopsis* RLK5 kinases (15.2–17.8 μM) (19, 21). Similar to CrRLK1 and the *Arabidopsis* BRI1 kinases, the activity of XA21K requires Mn^{2+} and Mg^{2+} but not Ca^{2+} (21, 22). These results suggest that autophosphorylation of XA21K may be an important step in the XA21-mediated signaling.

Intermolecular autophosphorylation is particularly important for activation of some RTKs that recognize growth factors in animal systems. Upon ligand binding, these RTKs form homodimers triggering intermolecular phosphorylation of regulatory residues that are essential for activation of the kinases (23). For example, the receptors for platelet-derived growth factor carrying intracellular tyrosine kinase domains are activated by dimerization of two receptors and subsequent intermolecular phosphorylation of the Tyr^{857} residue of the kinases. Here we report that autophosphorylation of XA21K occurs through an intramolecular mechanism. Furthermore, we were unable to detect *in vitro* intermolecular phosphorylation of the XA21K-K736E mutant protein by XA21K using either resin-bound or free fusion proteins. Similar systems were successfully used to demonstrate that XA21K can transphosphorylate one of the XA21-binding proteins.[2] Thus, our data suggest that intermolecular autophosphorylation is not the mechanism by which XA21K is activated. A possible mechanism for activation of the XA21K is that a second receptor kinase forms a heterodimer with and transphosphorylates XA21K following the infections of *Xanthomonas oryzae* pv. *oryzae,* which in turn activates the intramolecular autophosphorylation of XA21K.

Over the last decade, more than 20 plant disease-resistance genes have been cloned from a variety of plant species. Only the rice *Xa21* and tomato *Pto* resistance genes encode protein kinases. Although XA21K shares some common enzymatic properties with Pto, our studies also reveal that these two kinases likely employ distinct mechanisms for signaling. The phospho-

[2] L.-Y. Pi and W.-Y. Song, unpublished data.

rylation status in the activation domain of XA21K differs from that of the Pto kinase. Four of eight identified phosphorylation sites on Pto are located on the activation domain (12) (Fig. 7). One of them, Ser-198, is critical for avrPto-Pto-mediated elicitation of hypersensitive response. Like the Pto kinase, there are seven serine and threonine residues in the activation domain of XA21K (Fig. 7). Three of them are located in the corresponding positions (including Ser-198) of the Pto phosphorylation sites. However, our data suggest that none of these residues are autophosphorylated, indicating that phosphorylation of the activation domain may not be required for the XA21-mediated signaling. This is consistent with the observations from many other non-RD kinases that lack the conserved arginine preceding the conserved aspartate.

The RLK structure of XA21 suggests that the mode of action of this protein may be more similar to that of RTKs rather than Pto, a receptor-like cytoplasmic kinase (24). For instance, the extracellular domain of RTKs is required for ligand binding. Similarly, the presumed extracellular domain XA21 consists of LRRs that determines race-specific recognition of the pathogen (4). Furthermore, autophosphorylation of multiple tyrosine residues on the kinase domain of RTKs leads to initiation of multiple responses. A classic example is the platelet-derived growth factor receptor-mediated responses (23). Upon platelet-derived growth factor binding to its receptor, nine different tyrosine residues on the receptor are autophosphorylated, resulting in the recruitment of eight distinct intracellular signaling molecules. Because we have shown that XA21K can autophosphorylate multiple serine and threonine residues, it is possible that XA21 can initiate multiple defense responses by the binding of distinct signaling proteins with specific phosphorylated residues on XA21K. In support of this hypothesis, we have found that the active XA21K is capable of binding to at least seven rice proteins in the yeast two-hybrid system; however, these binding proteins showed either no or impaired interactions with the kinase-deficient mutant XA21K-K736E.[2] Thus, we propose that one function of the XA21K autophosphorylation is to create binding sites for recruiting downstream signaling proteins.

Acknowledgments—We thank Dr. H. C. Kistler for allowing use of his laboratory facility when W.-Y. S. started a new research program; we also thank Drs. Curtis L. Hannah, John Davis, and Pranjib K. Chakrabarty for critical reading of the manuscript.

REFERENCES

1. Flor, H. H. (1971) *Annu. Rev. Phytopathol.* **9,** 275–296
2. Staskawicz, B. J., Mudgett, M. B., Dangl, J. L., and Galan, J. E. (2001) *Science* **292,** 2285–2289
3. Dangl, J. L., and Jones, J. G. (2001) *Nature* **411,** 826–833
4. Wang, G.-L., Ruan, D. L., Song, W.-Y., Sideris, S., Chen, L., Pi, L.-Y., Zhang, S., Zhang, Z., Fauquet, C., Gaut, B. S., Whalen, M. C., and Ronald, P. C. (1998) *Plant Cell* **10,** 765–779
5. Xiao, S., Ellwood, S., Calis, O., Patrick, E., Li, T., Coleman, M., and Turner, J. G. (2001) *Science* **291,** 118–120
6. Martin, G. B., Brommonschenkel, S. H., Chunwongse, J., Frary, A., Ganal, M. W., Spivey, R., Wu, T., Earle, E. D., and Tanksley, S. D. (1993) *Science* **262,** 1432–1436
7. Ronald, P. C., Salmeron, J. S., Carland, F. M., and Staskawicz, B. J. (1992) *J. Bacteriol.* **174,** 1604–1611
8. Loh, Y.-T., and Martin, G. B. (1995) *Plant Physiol.* **108,** 1735–1739
9. Tang, X., Frederick, R. D., Zhou, J., Halterman, D. A., Jia, Y., and Martin, G. B. (1996) *Science* **274,** 2060–2062
10. Zhou, J., Loh, Y. T., Bressan, R. A., and Martin, G. B. (1995) *Cell* **83,** 925–935
11. Sessa, G., D'Ascenzo. M., Loh, Y.-T., and Martin, G. B. (1998) *J. Biol. Chem.* **273,** 15860–15865
12. Sessa, G., D'Ascenzo, M., and Martin, G. B. (2000) *EMBO J.* **19,** 2257–2269
13. Johnson, L. N., Noble, M. E. N., and Owen, D. J. (1996) *Cell* **85,** 149–158
14. Rathjen, J. P., Chang, J. H., Staskawicz, B. J., and Michelmore, R. W. (1999) *EMBO J.* **18,** 3232–3240
15. Song, W.-Y., Wang, G., Chen, L., Kim, H., Pi, L., Gardner, J., Wang, B., Holsten, T., Zhai, W., Zhu, L., Fauquet, C., and Ronald, P. C. (1995) *Science* **270,** 661–667
16. Ronald, P. C. (1997) *Plant Mol. Biol.* **35,** 179–186
17. Braun, D. M., Stone, J. M., and Walker, J. C. (1997) *Plant J.* **12,** 83–95
18. Deng, W. P., and Nickoloff, J. A. (1992) *Anal. Biochem.* **200,** 81–88
19. Horn, M. A., and Walker, J. C. (1994) *Biochim. Biophys. Acta* **1208,** 65–74
20. Levine, A., Tenhaken, R., Dixon, R., and Lamb, C. (1994) *Cell* **79,** 583–593
21. Schulze-Muth, P., Irmler, S., Schroder, G., and Schroder, J. (1996) *J. Biol. Chem.* **271,** 26684–26689
22. Oh, M. H., Ray, W. K., Huber, S. C., Asara, J. M., Gage, D. A., and Clouse, S. D. (2000) *Plant Physiol.* **124,** 751–766
23. Heldin, C. (1995) *Cell* **80,** 213–223
24. Shiu, S.-H., and Bleecker, A. B. (2001) *Proc. Natl. Acad. Sci. U. S. A.* **98,** 10763–10768